Energy Management Strategy for Wind Solar Storage Microgrid Based on Improved Ant Lion Optimizer

Rui Liu [a*]

[a] *School of Electric Power Engineering, Nanjing Institute of Technology, Nanjing-211167, China.*

Author's contribution

The sole author designed, analysed, interpreted and prepared the manuscript.

Original Research Article

ABSTRACT

The energy management of microgrids involves optimizing the capacity configuration, which significantly impacts the economic and stable operation of microgrids. This paper presents a control strategy for microgrid operation that effectively manages distributed power sources and energy storage to optimize capacity configuration. A mathematical optimization model for microgrid energy management is established considering minimum annual cost and optimal scale constraints. The traditional Ant Lion Optimizer (ALO) is improved by using dynamic weight coefficients and chaotic mapping to enhance the diversity of the population and improve the convergence of the algorithm. This can effectively avoid local optimal solutions and premature problems, and improve the convergence speed and search ability of the ALO algorithm. Based on this control strategy and improved ALO algorithm, simulations and tests were conducted using actual data from an independent microgrid, resulting in the optimal solution for the microgrid capacity allocation model. The case study results validate the practicality of the proposed microgrid operation control strategy as well as the superiority of the improved ant colony optimization algorithm.

_____

Corresponding author: E-mail: liurui20186@163.com;

1. INTRODUCTION

Microgrid is a kind of small power distribution system with high renewable energy penetration, which is composed of distributed power supply, energy storage system and load. As a distributed power management scheme, microgrid has become an important research direction of modern power grid, which can effectively solve the adverse problems that distributed power supply brings to the stability of distribution network due to the influence of natural environmental conditions. The microgrid energy management system can ensure the efficient operation of the microgrid, and build an effective management method for the distributed power supply, energy storage system and load part of the microgrid, which can ensure the maximum economic and environmental benefits of the microgrid [1-3].

The energy management of microgrid is to optimize the capacity allocation of microgrid. The energy management scheme has a great impact on the economy and stability of microgrid operation. At present, the main goal of the mainstream research is to build the model and optimize the algorithm [4-8].

The energy management of microgrid is to optimize the capacity allocation of microgrid, and the energy management scheme has a great impact on the economy and stability of microgrid operation. At present, the research is mainly on the model building and algorithm optimization with the goal of economy [9]. This paper proposes a double-layer energy optimal scheduling method of electric-hydrogen-thermal energy in park based on the alternating direction method of multipliers. By combining distributed and centralized energy, it realizes precise and optimal interaction of point-to-point energy of multiple subjects and low-carbon optimization [10]. The author first simulates the charging and discharging characteristics of a capacitor energy storage system, and then constructs a virtual energy storage system model incorporating multiple flexible resources, which is integrated into the DC microgrid. A two-layer scheduling framework is introduced to manage unplanned power fluctuations. To improve the reliability of microgrid operation, a regional coordinated control of short-term source load energy storage

based on virtual energy storage is proposed [11]. This paper proposes an independent microgrid system that combines a battery and a hydrogen storage system to improve energy efficiency. Using the improved multi-strategy Sparrow search algorithm (MSSA), a multi-objective optimization scheme with the lowest total investment cost and the lowest source load deviation rate is obtained [12]. An improved grey wolf optimization (IGWO) algorithm is proposed to determine the optimal combination of isolated island microgrids to achieve economic optimization. The optimization goal is to minimize the annual system cost, and the constraint is power supply reliability. The results show the effectiveness and applicability of this method [13]. A day-ahead scheduling strategy for microgrid energy storage system based on genetic algorithm and particle swarm optimization algorithm is proposed, aiming to reduce the total cost paid by users under dynamic electricity prices.

In this paper, on the one hand, the energy management optimization mathematical model of microgrid is established with the aim of minimizing the annual cost of the system, and on the other hand, the power capacity allocation of microgrid is studied considering the constraints of optimal scale. An operation design scheme of charge and discharge of energy storage is built, and the optimization problem of microgrid power supply is transformed into a nonlinear optimization problem. An improved Antlion algorithm based on dynamic weight coefficient and chaotic search is proposed to solve the problem. The final case study demonstrates the effectiveness of the method.

2. THE MATHEMATICAL MODEL OF EACH POWER SUPPLY IN MICROGRID

2.1 Photovoltaic System

The actual output power formula of photovoltaic panel (PV) [14] is shown in equation (1).

$$P_{\mathrm{PV}} = P_{\mathrm{STC}} \cdot G_C \frac{1 + h\left(T - T_{\mathrm{STC}}\right)}{G_{\mathrm{STC}}} \tag{1}$$

Where, P_{PV} is the actual output power of the operating point; P_{STC} is the rated output power of

PV under standard rated test conditions. G_C is the light intensity of the working point; h is the power temperature coefficient; T_{STC} is a reference temperature of 25℃; G_{STC} is the light intensity under standard conditions. T is the photovoltaic cell temperature; T_{at} is the ambient temperature, and its simplified mathematical formula is shown in equation (2).

$$T = T_{at} + 0.0254 G_C \qquad (2)$$

2.2 Wind Turbine Model

The actual output power equation of wind turbine (WT) [15] is shown in equation (3).

$$P_{WT} = \begin{cases} 0, 0 \le V \le V_{in} \\ P_r \dfrac{V - V_{in}}{V_r - V_{in}}, V_{in} \le V \le V_r \\ P_r, V_r \le V \le V_{out} \\ 0, V_{out} < V \end{cases} \qquad (3)$$

Where, V_{in} is the cut-in wind speed; V_r is rated wind speed; V_{out} is cut-out wind speed; P_r is the rated output power of wind turbine.

2.3 Energy Storage Model

In this paper, the battery is selected as the energy storage element, which can provide stable power to the load when the energy storage produces too much surplus energy and the renewable energy is short. The distributed power supply is easily affected by the environment and may produce excess or insufficient energy. The power equation of the battery to absorb and transport excess and insufficient energy is shown in equation (4).

$$P_b = P_{PV} + P_{WT} - \frac{P_L}{\eta} \qquad (4)$$

Where,

P_b is the power absorbed and transported by the battery; P_{PV} and P_{WT} are the total power generation of photovoltaic panels and wind turbines; P_L is the load demand; η indicates the inverter efficiency, which is 95%. When $P_b<0$, the generation loss is indicated, and when $P_b>0$, the

generation exceeds the demand. The State of Charge (SOC) of a battery is a parameter indicating the ratio of the remaining capacity of the battery pack to the capacity of the fully charged state. The charge and discharge calculation formula [16] are shown in equation (5)-(6).

$$SOC(t) = SOC(t-1) \times (1-\sigma) + \left[P_{PV}(t) + P_{WT}(t) - \frac{P_L}{\eta} \right] \times \eta_B \qquad (5)$$

$$SOC(t) = SOC(t-1) \times (1-\sigma) + \left[\frac{P_L}{\eta} - P_{PV}(t) - P_{WT}(t) \right] \times \eta_B \qquad (6)$$

Where,

σ is the self-discharge efficiency; η_B is the cell efficiency; η is inverter efficiency.

2.4 Diesel Generator Model

When the battery is exhausted or the load peaks, the diesel generator can be used as the secondary power supply of the microgrid. Its model is based on fuel consumption and efficiency, and the output power formula is shown as equation (7) [17].

$$F_D = \alpha P_{DG} + \beta P_r \qquad (7)$$

Where,

F_D is fuel consumption; P_{DG} is power generation; P_r is the rated power, α and β are the coefficients.

3. ENERGY STORAGE CHARGING AND DISCHARGING STRATEGY

Renewable energy is characterized by randomness and intermittence under the influence of natural environment. Therefore, it is considered to set the operation control strategy of microgrid to realize the effective control and management of distributed power supply, energy storage and load. The charging state of the energy storage is related to its charging and discharging power, and a reasonable charging and discharging standard can avoid frequent deep charging and discharging process, prevent damage to the energy storage device and prolong the life of the device. The difference between renewable energy and load power is shown in equation (8).

$$\Delta P = P_{\text{WT}} + P_{\text{PV}} - \frac{P_{\text{L}}}{\eta} \qquad (8)$$

According to the charged state of the energy storage, when ΔP is greater than 0 and the energy storage is not fully charged, the remaining energy generated will charge the energy storage. When ΔP is greater than 0 and the energy storage is full, properly discard wind and light to prevent the energy storage from overcharging. When ΔP is less than 0, the generation is less than the load demand. If the state of energy storage charge is greater than the minimum value, discharge is performed. If it is lower than the lowest value of the charged state, the discharge rate is 0, that is, no discharge. The charge and discharge flow chart of energy storage is shown in Fig. 1. E_{b} is the energy stored by the battery, E_{c} is the energy charged by the battery, E_{dc} is the discharge energy, and P_{E} is the charge and discharge power of the battery.
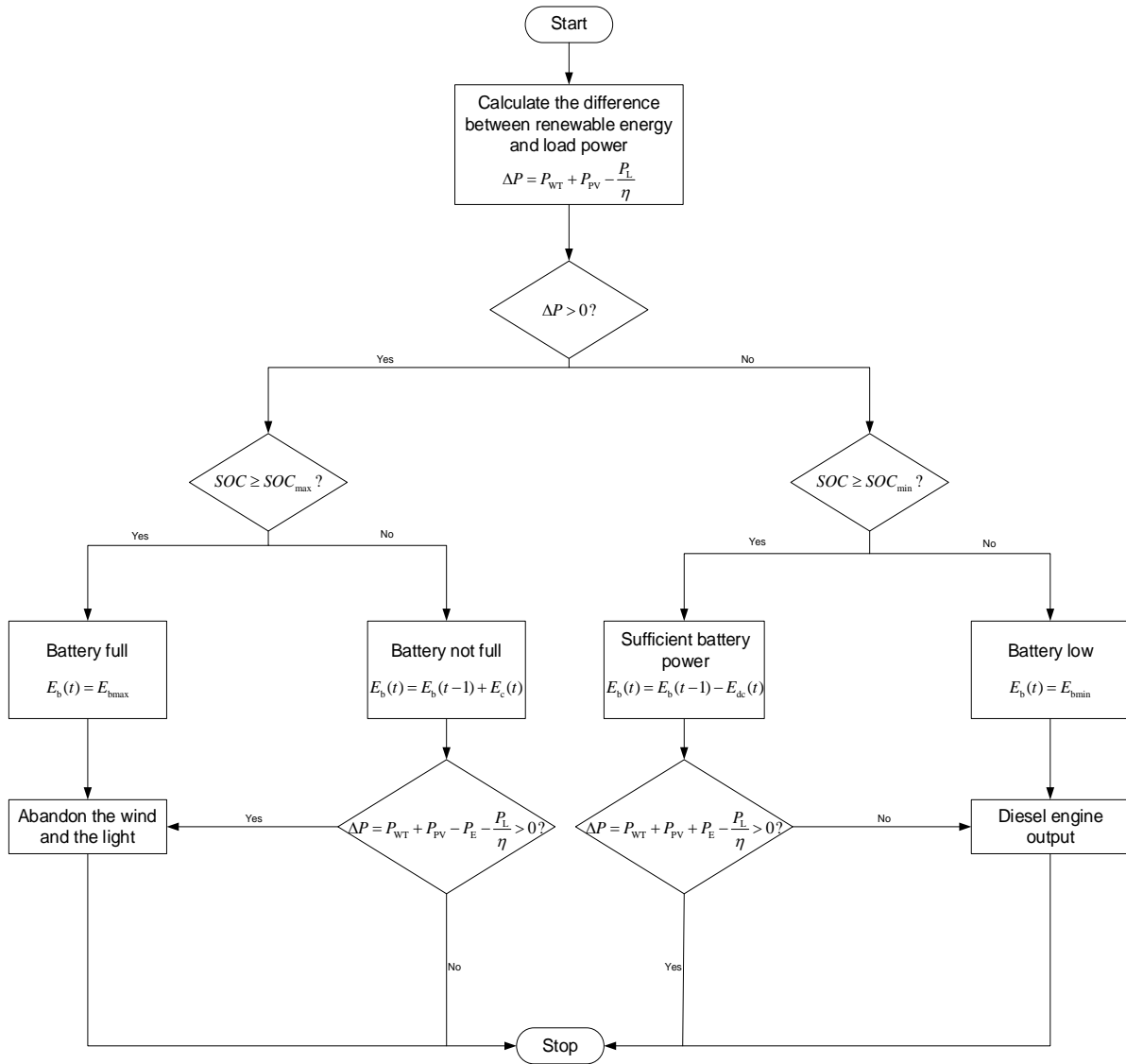

Fig. 1. Charge and discharge flow chart of energy storage

4. POWER SUPPLY OPTIMIZATION CONFIGURATION MODEL

4.1 Objective Function

In this paper, the capacity allocation optimization model of microgrid is established to minimize the annual comprehensive investment cost of the system, including investment cost, replacement cost, operation and maintenance cost and fuel cost. The objective function equation is shown in equation (9)-(13).

$$F = \sum_{i=1}^{N} \left[C_{\text{in},i} + C_{\text{re},i} + C_{\text{om},i} + C_{\text{fc},i} \right] \tag{9}$$

$$C_{\text{in},i} = C_{\text{ca}} \times \frac{r(1+r)^{LP}}{(1+r)^{LP} - 1} \tag{10}$$

$$C_{\text{re},i} = C_{\text{Bre}} \times \frac{r}{(1+r)^{Y} - 1} \tag{11}$$

$$C_{\text{om},i} = C_{\text{ca}} \times K_{\text{om}} \tag{12}$$

$$C_{\text{fc},i} = C_{\text{f}} \times F_{\text{D}} \tag{13}$$

Where, N is the number of power supplies; $C_{in,i}$ is the investment cost of the i power supply; $C_{re,i}$ is the replacement cost of type i power supply; $C_{om,i}$ is the operation and maintenance cost of the i power supply; $C_{fc,i}$ is the fuel cost of the i power supply; C_{ca} is the capital cost of equipment; r is the interest rate; LP is the system lifetime; C_{Bre} for battery replacement costs; Y is battery life; K_{om} is the proportional coefficient of power operation and maintenance cost; C_f is the fuel cost of diesel generator set.

4.2 System Power Balance and Constraints

4.2.1 System power balance

To maintain power balance between the generation side and the load demand side, the following formula should be met.

$$P_{\text{L}} = P_{\text{WT}} + P_{\text{PV}} + P_{\text{DG}} + P_{\text{E}} \tag{14}$$

4.2.2 Battery constraints

The charge and discharge of the battery need to be restricted, which can effectively ensure the service life of the energy storage. The formula is shown in equation (15).

$$SOC_{\min} \leq SOC \leq SOC_{\max} \tag{15}$$

Where, SOC is the charge amount of the battery, SOC_{max} and SOC_{min} are the upper and lower limits of the battery capacity respectively.

4.2.3 Diesel engine constraint

The diesel generator constraint formula is shown in equation (16).

$$P_{\text{DGmin}} \leq P_{\text{DG}} \leq P_{\text{DGmax}} \tag{16}$$

Where, P_{DGmax} and P_{DGmin} are the upper and lower limits of the power of the diesel generator respectively.

5. IMPROVED ANT LION OPTIMIZER

Ant Lion Optimizer [18] is a meta-heuristic algorithm proposed by Mirjalili in 2015 based on the behavior of ant lions making traps to prey on ants. The algorithm simulates the interaction between antlion and ant in the trap.

Since the walking motion of ants when searching for food is random, the random walk is used to simulate its movement, and the formula is shown as equation (17).

$$X(t) = [0, \ cumsum(2r(t_1)-1), L \ , cumsum(2r(t_n)-1)] \tag{17}$$

Where, $cumsum$ is the cumulative sum, n is the maximum number of iterations, t_1 to t_n is the random walk length of ants, which is iteration in ALO, $r(t)$ is a random function, and the formula is shown as equation (18).

$$r(t) = \begin{cases} 1, & \text{if } rand > 5 \\ 0, & \text{if } rand \leq 0.5 \end{cases} \tag{18}$$

Where, $rand$ is a random number that is uniformly distributed between [0, 1].

Ant's random walk needs to be constrained, and the constrained walk equation is shown in equation (19).

$$X_i^t = \frac{(X_i^t - a_i) \times (d_i - c_i^t)}{(d_i^t - a_i)} + c_i \tag{19}$$

Where, a_i is the minimum random walk of the i th variable, d_i is the maximum random walk of the i th variable, $ct\ i$ is the minimum value of the i th variable in the t th iteration, and $dt\ i$ is the

maximum value of the i variable in the t th iteration.

The equation that changed when the ants were disturbed was as follows:

$$c_i^t = Antlion_j^t + c^t \qquad (20)$$

$$d_i^t = Antlion_j^t + d^t \qquad (21)$$

Where, c^t is the smallest variable at the t iteration and d^t is the largest variable at the t iteration. $ct\ i$ is the smallest variable for the i th ant and $dt\ i$ is the largest variable for the i th ant. $Antliont\ j$ is the position of the j th antlion on the t iteration.

Since the antlion can build traps proportional to its fitness to hunt ants, and because ants need to be on the move at any time, when the antlion detects the presence of ants in the trap, it shoots sand from the pit at the ants as they attempt to escape. The following equation was used for mathematical modeling of the ant lion's behavior, and the random walking radius of the ant was adaptively reduced, as shown in equation (22)-(23).

$$c^t = \frac{c^t}{I} \qquad (22)$$

$$d^t = \frac{d^t}{I} \qquad (23)$$

Where, c^t represents the minimum value of all variables at the t-th iteration, and d^t represents the vector containing the maximum value of all vectors at the t-th iteration. I is the ratio, as shown in equation (24).

$$I = 10^w \frac{t}{T}, w = \begin{cases} 2, t > 0.1T \\ 3, t > 0.5T \\ 4, t > 0.75T \\ 5, t > 0.9T \\ 6, t > 0.95T \end{cases} \qquad (24)$$

Where t is the current iteration, T is the maximum number of iterations, and w is the constant based on the current iteration.

When the ant lion successfully preys on ants, it needs to update its latest position so as to increase the chance of catching new prey later,

and this behavior is modeled mathematically, as shown in Equation (25).

$$Antlion_j^t = Ant_i^t \text{ if } f(Ant_i^t) > f(Antlion_j^t) \qquad (25)$$

Where t represents the current iteration, $Antliont\ j$ is the position of the j th antlion selected in the t iteration, and $Antt\ i$ is the position of the i ant in the t iteration.

The elite strategy in the intelligent evolutionary algorithm can keep obtaining the best solution. The optimal antlion results are saved, and the equation of ants affected by the optimal results is shown in equation (26).

$$Ant_i^t = \frac{R_A^t + R_E^t}{2} \qquad (26)$$

Where, $Rt\ A$ is the random walk of the selected ant at the t iteration, $Rt\ E$ is the random walk of the elite at the t iteration, and $Antt\ i$ is the position of the i ant at the t iteration.

ALO has the ability of global and local search, but it is easy to encounter the problem of local optimal solution when dealing with more complex functions. This may cause the algorithm to fail to find the global optimal solution. And when the problem size is large or the solution space is complex, the convergence speed of Antlion algorithm may be slow. To solve the above problems, this paper adopts the improved strategies of dynamic weight coefficient and chaotic search to increase the diversity of the population, improve the optimization and search ability of the algorithm, and avoid the problem that the local optimal solution and the convergence may be slow when processing complex function models.

5.1 Dynamic Weight Coefficient

The dynamic weight coefficient can be dynamically adjusted according to the different stages of the iterative process, so that the algorithm pays attention to the global search at the initial stage of the search, and it is convenient to search the optimal solution region. In the later stage of the algorithm search, we pay more attention to local search, so that we can carry out fine search positioning in the optimal solution region and find the optimal solution.

In formula 27, the position of the i ant in the t iteration can be further rewritten as:
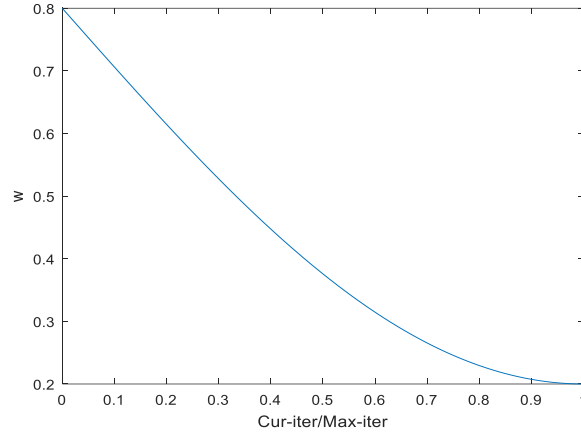
Fig. 2. Weight coefficient curve

$$Ant_i^t = wR_A^t + (1-w)R_E^t \qquad (27)$$

In the original formula, *w* is 0.5. In all iterations, the random walks of the ant and the elite antlion are weighted the same, and the algorithm cannot be dynamically adjusted according to different stages of the iterative process. Therefore, this paper proposes to change the weight coefficient, and by dynamically adjusting the weight coefficient, the algorithm can avoid the problem of local optimal solution to a certain extent. *w* is shown in formula (28).

$$w = \frac{4}{5} - \frac{3}{5}\sin(Cur\_iter / Max\_iter * pi / 2) \qquad (28)$$

Where *Cur_iter* is the current iteration number and *Max_iter* is the maximum iteration number. The weight coefficient curve is shown in Fig. 2.

5.2 Tent Mapping

Using Tent chaotic mapping as the chaotic sequence to generate the optimization algorithm can maintain the diversity of the initial population and avoid the algorithm falling into the local optimal solution, thus improving the optimization speed and search ability of the algorithm. The Tent mapping formula is shown in Equation (29) [19].

$$x_{t+1} = \begin{cases} 2x_t, & 0 \le x_t \le 0.5 \\ 2(1-x_t), & 0.5 \le x_t \le 1 \end{cases} \qquad (29)$$

5.3 Cubic Mapping

Cubic mapping is a chaotic mapping with simple structure and complex dynamic behavior. The standard Cubic mapping is shown in equation (30) [20].

$$x_{n+1} = \xi x_n^3 - (\xi - 1)x_n \qquad (30)$$

Where *r* is the influence factor, $x_n \in (-1,1]$, the Cubic mapping sequence is chaotic when $\xi \in [3.3,4]$. In this paper, $\xi=3.69$ is selected, in which case the algorithm has good ergodicity.

6. MICROGRID OPTIMIZATION CONFIGURATION PROCESS

The flowchart for the capacity configuration of microgrids using the improved antlion algorithm is shown in Fig. 3. The configuration steps are as follows:

- Initialize variables and set parameters.
- Input meteorological and load data for the microgrid location, and calculate the output of distributed power sources.
- Generate the initial populations of antlions and ants using Tent mapping.
- Calculate the fitness values of the initial antlions and sort them.
- Update the random walk of elite antlions.
- Check for boundary violations in antlion movement, bringing back any out-of-bounds individuals within search boundaries.
- Update the position and fitness of antlions using Cubic mapping and ants.
- Update the latest position of elite antlions.

21
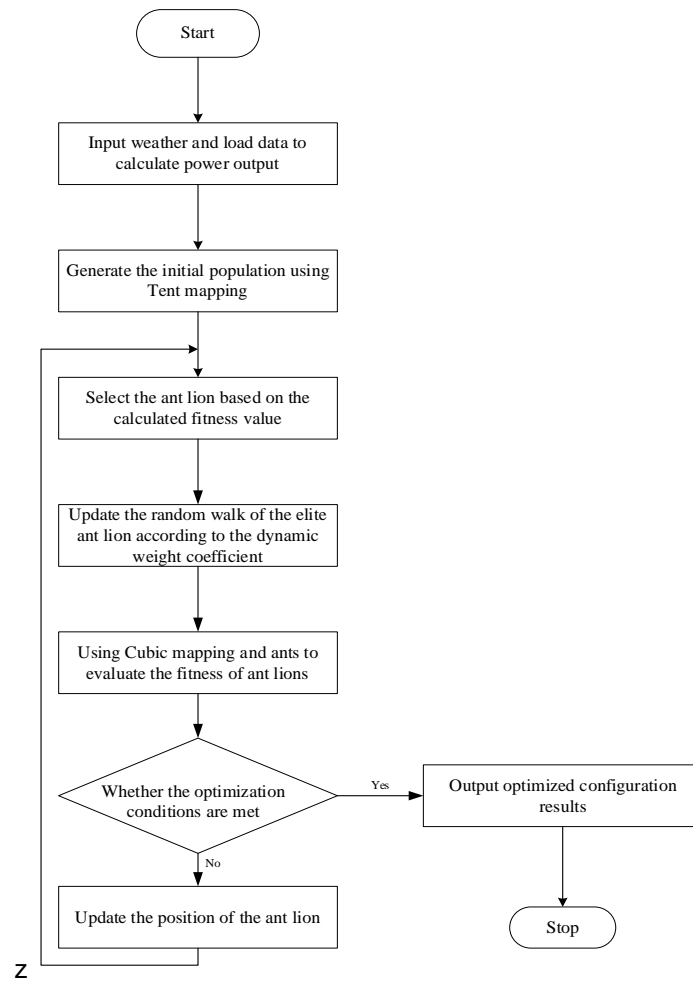
Fig. 3. Flow chart of microgrid capacity configuration based on ALO
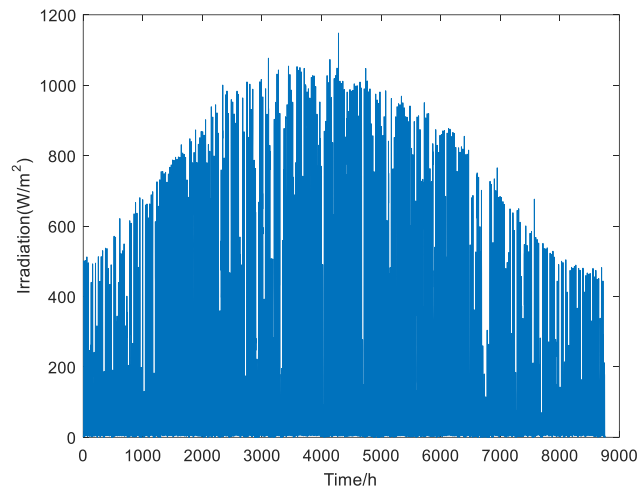
7. CASE STUDY

The following uses the microgrid operation control strategy and configuration mathematical model proposed in this paper to simulate the microgrid in a certain area. Taking meteorological and load data as input, the actual meteorological data and load data of this region are shown in Fig. 4.
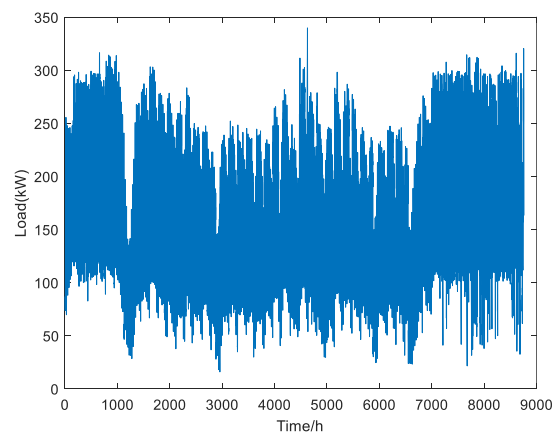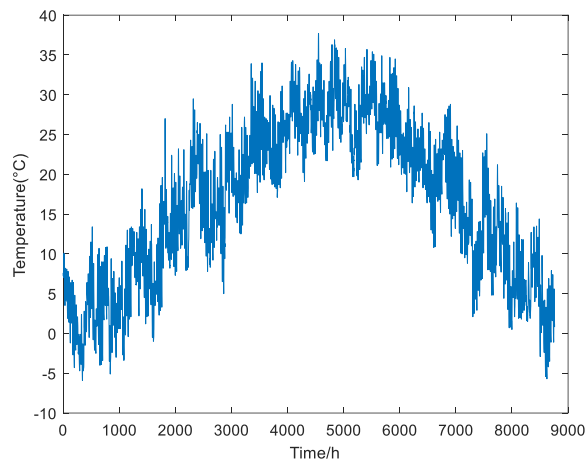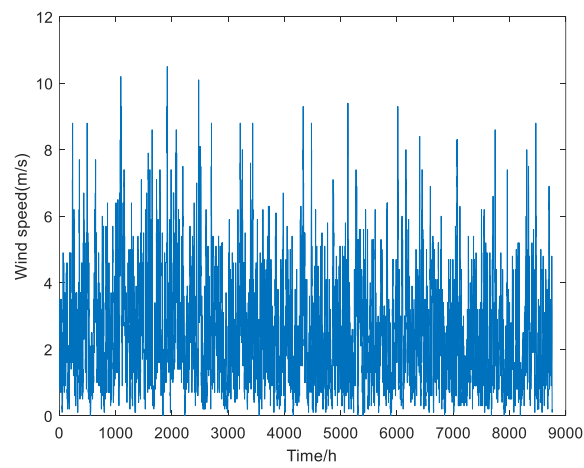

(a) Hourly load throughout the year

22

(b) Hourly light throughout the year

(c) Annual hourly temperature

(d)

(e) Hourly wind speed throughout the year

Fig. 4. Meteorological data and load data

Table 1. Cost of distributed power generation units

| Distributed power supply	capital cost/$	Installation cost/$	Operation and maintenance cost/$	Replacement cost/$	durable years/$
WT	4960	2980	12	0	20
PV	3000	1000	8.2	0	20
Battery	1000	200	6.3	200	3
Diesel generator	4300	1000	374	0	20

According to the optimization model and constraint conditions established in this paper, the capacity allocation of microgrid is optimized. Set the population number to 30, the maximum number of iterations to 100, the interest rate r=0.067, the system life LP=20, and the battery life Y=3. The rated capacity of the battery is 200A·h, and the maximum charge and discharge power is 10kW. The range constraint of the energy storage is between 0.1 and 0.9, with an initial value of 0.5. The types of power supplies simulated in this paper include fan, photovoltaic array, storage battery and diesel generator. Unit costs of each power supply are shown in Table 1.

According to the operation control strategy proposed in this paper, simulation results of SOC changes on a typical day are shown in Fig. 5. The SOC is between 0.1 and 0.9, and it can be seen from Fig. 5 that the SOC changes have been within the specified constraint range. As shown in Fig. 6, when the WT output is high from 0 to 10, the difference between renewable energy and load ΔP is greater than 0 and the energy storage is not fully charged, the remaining energy will be charged to the energy storage. From 10 to 19 o 'clock, the light intensity increases, the PV output increases, and the energy storage charging reaches a peak. When the night light reduction is close to 0, the photovoltaic output is far reduced. The energy storage starts to discharge to maintain the power balance of the system, and the energy storage self-discharge to the lowest constraint after 22 o 'clock. The rapid change of SOC during this period ensures the discharge of energy storage and the power balance of the system.
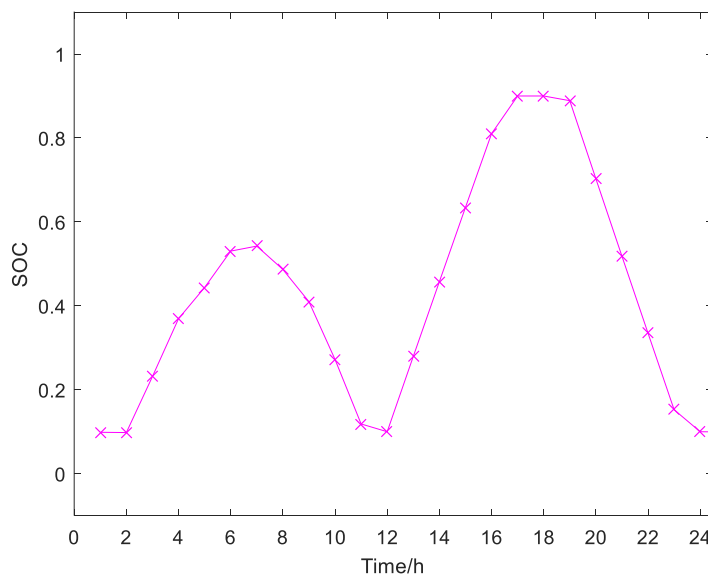

Fig. 5. SOC curve
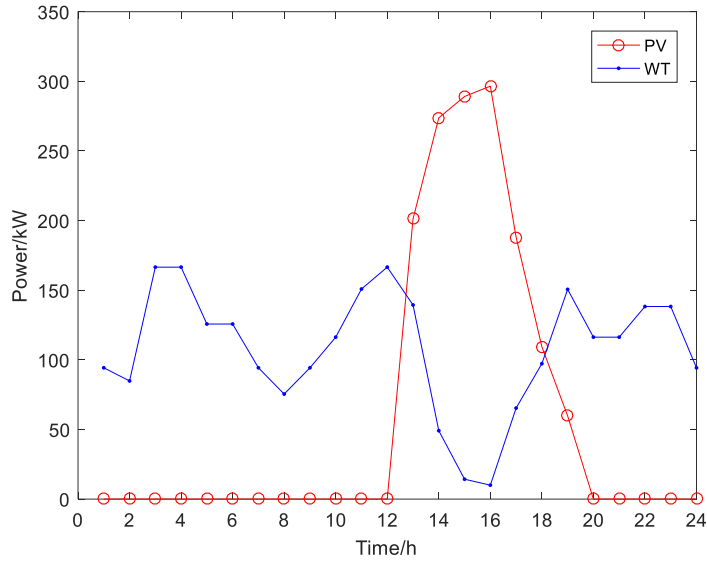
Fig. 6. Photovoltaic and wind turbine generator output

The output and load power data of each unit in four typical weeks of spring, summer, autumn and winter in a year are selected to verify the feasibility and effectiveness of the operation control strategy proposed in this paper, and the results are shown in Fig. 7. According to the hourly meteorological data throughout the year, the light intensity and climate temperature in summer and autumn are much higher than that in spring and winter, so the PV output is much higher than that of the WT. This is most evident during the summer week, when the average difference between PV and fan output is 131.198kW, while the winter week difference is only 73.144kW. The energy storage changes within the prescribed constraint range to meet the changing requirements of load power and maintain the power balance of the system. The results show that the operation strategy can realize the rational control and management of power supply, energy storage and load.
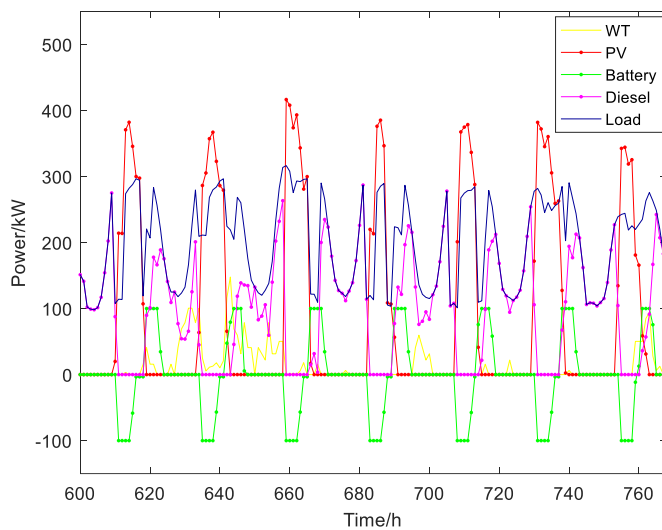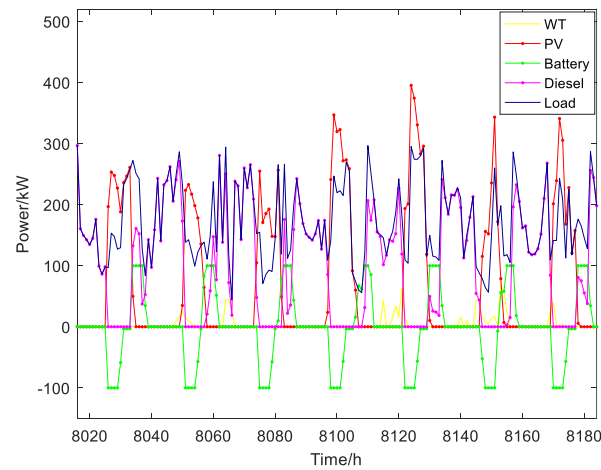

(a) Spring weekly unit and load power
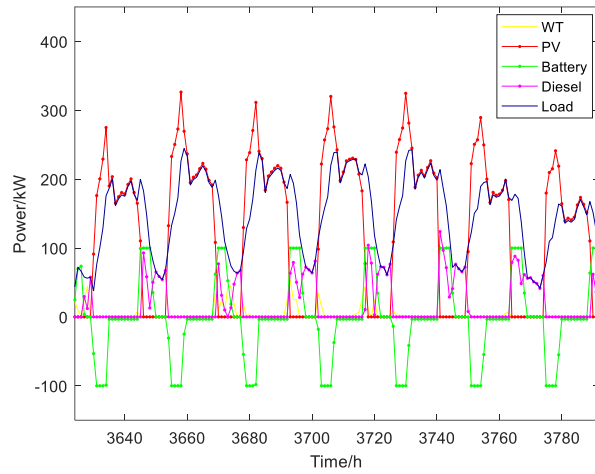
(b) Summer weekly unit and load power
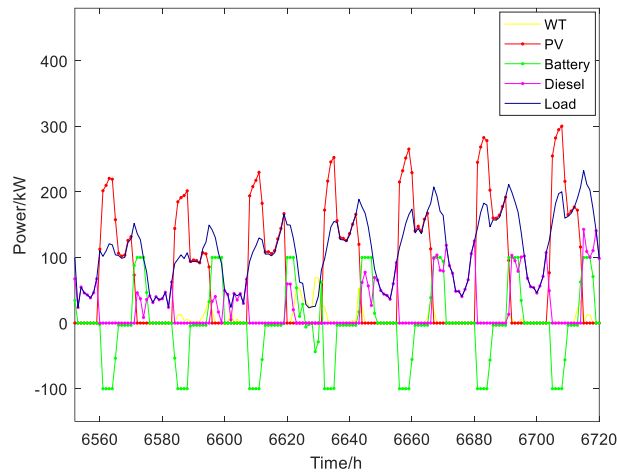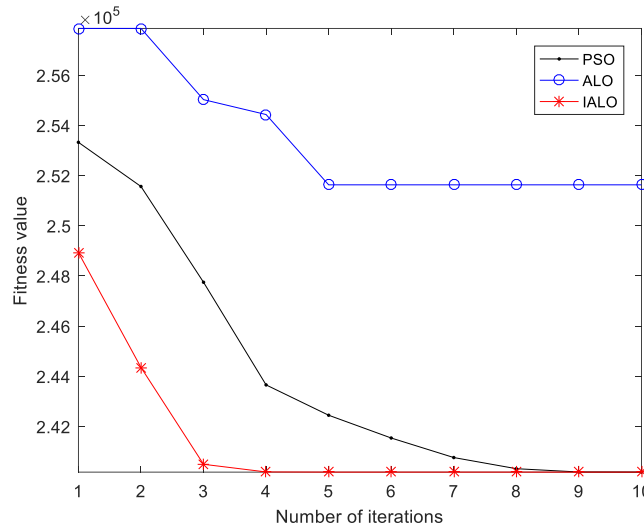

(c) Autumn weekly unit and load power

(d) Winter weekly unit and load power

Fig. 7. Typical weekly unit and load power in different seasons

Table 2. Microgrid capacity configuration scheme

scheme	WT	PV	Battery	Diesel	cost/$
1	0	7	10	6	244463
2	50	0	0	6	409976
3	21	6	10	6	242544

Fig. 8. Convergence curves of ALO, IALO and PSO

Three power supply configuration schemes are designed to analyze the capacity configuration model of independent microgrid. Add the penalty cost of wind and light abandonment, calculate by the improved Antlion algorithm, and the capacity configuration results of the microgrid are shown in Table 2.

According to the comparison and analysis of Table 2, Scheme 2 only has WT and Diesel generator, and due to the excessive output of Diesel generator, the comprehensive cost is high. Plan 1 is missing WT, and the price of capacity configuration results in an increase. Scheme 3 has a higher utilization rate of renewable energy compared with other schemes, and the comprehensive cost after optimization by the algorithm is reduced by 0.78% compared with scheme 1, becoming the optimal combination scheme.

Ordinary ALO, improved ALO and Particle Swarm Optimization were used to perform optimization calculations. The comparison of iterative curves of the results of each algorithm is shown in Fig. 8. Fig. 8 shows that the Antlion algorithm with improved dynamic weight coefficient and chaotic search has faster convergence speed and better optimization accuracy than the traditional ALO and PSO, which can avoid falling into the local optimal solution and has better search ability.

8. CONCLUSION

The capacity allocation model of microgrid proposed in this paper takes the minimum annual cost of the system as the optimization objective and considers the constraints of the optimal scale. A microgrid operation strategy scheme is developed to ensure the stable operation of the system and realize reasonable control and management. An improved ALO is proposed for capacity allocation optimization, which adopts dynamic weight coefficient and chaotic mapping, and compares with ALO and PSO. The results show that the improved ALO has better convergence speed and accuracy. The improved ALO is used to calculate the capacity configuration of microgrid, solve the proposed model, and get the optimal configuration scheme.

DISCLAIMER (ARTIFICIAL INTELLIGENCE)

Author(s) hereby declare that NO generative AI technologies such as Large Language Models (ChatGPT, COPILOT, etc) and text-to-image

generators have been used during writing or editing of manuscripts.

ACKNOWLEDGEMENTS

COMPETING INTERESTS

Author has declared that no competing interests exist.

REFERENCES

1. Lu Zongxiang, Wang Caixia, Min Yong, et al. Overview on microgrid research[J]. Automation of Electric Power Systems. 2007;(19):100-107.
2. Yang Xinfa, Su Jian, Lü Zhipeng, et al. Overview on micro-grid technology[J/OL]. Proceedings of the CSEE. 2014;34(1):57-70.
3. Wang Chenshan, Li Peng. Development and challenges of distributed generation, the micro-grid and smart distribution system[J]. Automation of Electric Power Systems. 2010;34(2):10-14+23.
4. Roy K, Mandal KK, Mandal AC. Ant-Lion Optimizer algorithm and recurrent neural network for energy management of micro grid connected system. Energy. 2019, Jan 15;167:402-16.
5. Fathy A, Kaaniche K, Alanazi TM. Recent approach based social spider optimizer for optimal sizing of hybrid PV/wind/battery/diesel integrated microgrid in aljouf region. IEEE Access. 2020, Mar 23;8:57630-45.
6. Hajizadeh M, Gharehpetian GB, Ghassemzadeh S, Askari MT. Optimal eco-emission scheduling of demand and supply side of microgrids using multi-objective ant lion optimization and fuzzy decision-making. Electric Power Components and Systems. 2022, Jan 20;50(1-2):52-63.
7. Lotfy Haridy A, Ali Mohamed Abdelbasset AA, Mohamed Hemeida A, Mohamed Ali Elhalwany Z. Optimum controller design using the ant lion optimizer for PMSG driven by wind energy. Journal of Electrical Engineering & Technology. 2021, Jan;16:367-80.
8. Nair RP, Kanakasabapathy P. PR controller-based droop control strategy for AC microgrid using Ant Lion Optimization technique. Energy Reports. 2023, Dec 1;9:6189-98.
9. Kong Lingguo, Shi Lihao, Shi Zhenyu, et al. Low-carbon optimal dispatch of electric-hydrogen-heat system in park based on alternating direction method of multipliers[J/OL]. Transactions of China Electrotechnical Society. 2023;38(11):2932-2944.
10. Zhang Xiangyu, Shu Yinan, Fu Yuan. Multi-time-scale energy optimization and zone coordinated control of dc microgrid source-load-storage based on virtual energy storage[J/OL]. Transactions of China Electrotechnical Society. 2022; 37(23):6011-6024.
11. Zhang Ping, Lu Xia, Meng Qinghe. Optimal allocation of micro-grid capacity based on multi-strategy sparrow search algorithm[J]. Electrical Engineering. 2023; 24(1):1-9.
12. Zhao Chao, Wang Bin, Sun Zhixin, et al. Optimal configuration optimization of islanded microgrid using improved grey wolf optimizer algorithm[J/OL]. Acta Energiae Solaris Sinica. 2022;43(1):256-262.
13. Raghavan A, Maan P, Shenoy AKB. Optimization of day-ahead energy storage system scheduling in microgrid using genetic algorithm and particle swarm optimization[J/OL]. IEEE Access. 2020;8: 173068-173078.
14. Chen H, Gao L, Zhang Z, et al. Optimal energy management strategy for an islanded microgrid with hybrid energy storage[J/OL]. Journal of Electrical Engineering & Technology. 2021;16(3): 1313-1325.
15. Li Yanzhe, Guo Xiaojia, Dong Haiying, et al. Optimal capacity configuration of wind/pv/storage hybrid energy storage system in microgrid[J/OL]. Proceedings of the CSU-EPSA. 2020; 32(6):123-128.
16. Zeng J, Wang Q, Liu J, et al. A Potential game approach to distributed operational optimization for microgrid energy management with renewable energy and demand response[J/OL]. IEEE Transactions on Industrial Electronics. 2019;66(6):4479-4489.
17. Cetinbas I, Tamyurek B, Demirtas M. The hybrid harris hawks optimizer-arithmetic optimization algorithm: A new hybrid algorithm for sizing optimization and

design of microgrids[J/OL]. IEEE Access. 2022;10:19254-19283.

18. Mirjalili S. The ant lion optimizer[J/OL]. Advances in Engineering Software. 2015; 83:80-98.

19. Teng Zhijun, Lü Jinling, Guo Liwen, et al. An improved hybrid grey wolf optimization algorithm based on Tent mapping[J].

Journal of Harbin Institute of Technology. 2018;50(11):40-49.

20. Zhang Meng-jian, Zhang Hao, Chen Xi, et al. A grey wolf optimization algorithm based on Cubic mapping and its application[J]. Computer Engineering & Science. 2021;43(11):2035-2042.